

Article

A Novel Fabrication of Spherical Fe₅₀Ni₅₀ Alloy Powders via in-Situ De-Wetting of Liquid Solid Interface

Xueyin Song ¹, Chenglong Lei ^{2,3,*} and Wei Zhong ^{1,*}

¹ Collaborative Innovation Center of Advanced Microstructures, National Laboratory of Solid State Microstructures and Jiangsu Provincial Laboratory for NanoTechnology, Nanjing University, Nanjing 210093, China; songxueyin@126.com

² College of Engineering and Applied Science, Nanjing University, Nanjing 210093, China

³ Haian Institute of High-Tech Research, Nanjing University, Nanjing 226600, China

* Correspondence: leichenglong@nju.edu.cn (C.L.); wzhong@nju.edu.cn (W.Z.)

Received: 28 May 2019; Accepted: 23 June 2019; Published: 26 June 2019

Abstract: Spherical Fe₅₀Ni₅₀ alloy powders were fabricated via a novel route based on in-situ interface de-wetting between liquid Fe-Ni alloy and alumina. The obtained Fe₅₀Ni₅₀ alloy particles exhibit very good spherical shape according to SEM images. Furthermore, the cross-sectional SEM images show that there are no pores and bulk inclusions in the internal region of the spherical particles. The XRD results show a trace amount of the impurity alumina phase appearing in taenite phase. The size distribution agreed well with the SEM observation confirms that the alumina powders successfully segregated pre-alloy powders. As an incidental benefit, the surface alumina particles were treated as the electrical insulation coatings. The magnetic character shows that spherical Fe₅₀Ni₅₀ powders exhibit a good soft magnetic property even though with a slightly decreasing of saturation magnetization due to non-magnetic coatings. Our strategies provide a method to in-situ fabricate insulation coated Fe-Ni spherical alloy powders as magnetic powder core.

Keywords: spherical Fe-Ni powders; de-wetting; alumina; liquid-solid interface; magnetic properties

1. Introduction

Soft magnetic alloys and compounds show great potential applications in the field of electronic and energy conversion devices [1,2]. In a variety of soft magnetic materials, Fe-Ni alloy shows many advantages in magnetic performances, such as high permeability, high saturation induction and low coercive force [3,4]. Recently, many works are focused on the fabrication of soft magnetic cores using a powder process for reducing eddy current loss effectively. As an electromagnetic device under high frequencies, the inner region of magnetic powder will form small units by the introduction of electrical insulation [5,6]. Unfortunately, the undesirability of electrical insulation also shows some disadvantage for magnetic powder with edges and corners, resulting in the increase of magnetic core loss. Therefore, those alloy powders with good spherical shape have attracted much attention for electrical insulation in powder metallurgy.

Nowadays, the preparation of ultrafine Fe-Ni alloy powders is carried out by the solution phase route, including reduction in aqueous solution, sol-gel method followed by H₂ reduction and hydrothermal reduction [1,7–9]. Considering the narrow size distribution and large scale produce, ultrafine alloy powder was often fabricated in industry by mixing with some metal oxide powders and by using the hydrogen reduction method [4,7]. In order to reduce the agglomeration of the particle, metalloid solid materials are introduced as an agglomeration preventive-medium. It is a

low-cost process for fabricating morphology-controlled powders in large scale and optimizing the parameters at industry conditions [10,11]. However, Fe-Ni alloy powders that are nanosized are only prepared in lab scale, which cannot meet the needs of industry at low cost. In addition, the method for fabricating spherical Fe-Ni alloy powders has been reported less except for gas atomization. In the last few decades, based on surface tension principles, the metal droplet was often obtained for preparing spherical metal powder in a gas medium (i.e., the liquid/gas interface) [3,12], or in the liquid medium (i.e., the liquid/liquid interface) [13]. However, a solid medium surface will have wetting or de-wetting (e.g., atoms diffusion and cluster nucleation), resulting in interactions of the liquid/solid interface [14,15]. Therefore, it is still a great challenge to fabricate spherical alloy powders using the surface tension principles of a metal droplet dispersed in a solid medium (i.e., the liquid/solid interface).

In this work, the spherical Fe₅₀Ni₅₀ alloy powders fabricated using the surface tension principles on a liquid-solid interface was reported. Alumina medium was used as an isolation material. It is a proof-of-concept of a “solid solution” in terms of the de-wetting of alumina for spherical Fe₅₀Ni₅₀ powders. Due to de-wetting, the in situ separation between the alloy particle and alumina may occur, which mainly enrich the surface of alloy powders. As an incidental benefit, the surface alumina serves as the electrical insulation coatings for Fe₅₀Ni₅₀ alloy powders.

2. Experiment Procedure

Ferric nitrate (AR, 99.9%) and nickel nitrate (AR, 99.9%) were used as the source of Fe and Ni to prepare Fe₅₀Ni₅₀ alloy powders. The mixture metal oxides were obtained via a co-precipitation method by rapidly adding NaOH solution into the nitrate salts transparent aqueous solution. The precursor was formed after vacuum suction filtration and drying. Spherical Fe₅₀Ni₅₀ alloy powders were fabricated via two steps: (1) Pre-alloy experiments were carried out at 973 K for 1h in an open quartz tube with an inner diameter 5 cm via route one shown in Fig.1. The mixture metal oxides were scattered in sodium chloride (NaCl) by mixing for approximately 30 min, with the mass ratio of 1:3. After reducing and subsequently removing NaCl, the ultrafine pre-alloy powders of Fe₅₀Ni₅₀ were obtained. (2) The spheroidizing of Fe₅₀Ni₅₀ alloy powders were carried out by route two (shown in Figure 1) that pre-alloy powders were scattered in ultrafine alumina (1 μm, 99%) again and heated to molten state at 1823 K for 10 min and subsequently cooled to room temperature. The spherical powders were collected by a combination of the ultrasonic and magnetic separation in aqueous solution. SEM and energy dispersive spectrometer (EDS) were used to observe the surface morphology and composition analysis of the spherical powder by scanning electron microscopy (SEM, Hitachi S3400, Hitachi Ltd., Chiyoda-ku, Japan) using an instrument and energy dispersive spectrometer (EDS). The size-distribution of spherical powder was measured by laser diffraction (Mastersizer 3000, Malvern Instruments Ltd, Worcestershire, UK). The XRD patterns were obtained via an X-ray diffraction (Bruker D8, Bruker AXS GmbH, Bruker, Germany) using Cu-Kα radiation (λ=1.5406Å). The vibrating sample magnetometer (VSM, Lakeshore Model 7300, Lakeshore Instruments, Columbus, Ohio, USA) was used to measure Room temperature hysteresis (M–H) loops.

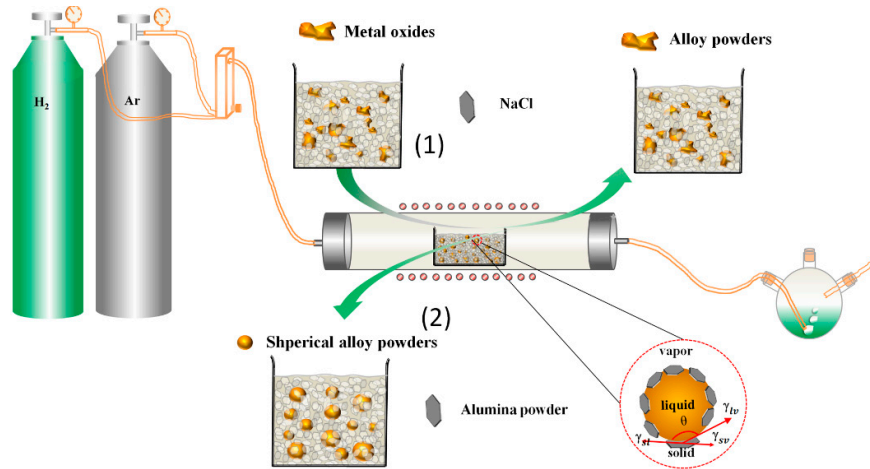


Figure 1. Schematic illustration of (1) pre-alloy from the reduction of mixed metallic oxides on NaCl, (2) spherical alloy powders fabricated at 1823 K on alumina, enlarged view of the triple solid–liquid–vapor junction of metal droplet.

3. Results and Discussion

Figure 2 shows the SEM micrograph of pre-alloy and spherical $\text{Fe}_{50}\text{Ni}_{50}$ alloy powders. The morphology of pre-alloy by the hydrogen reduction in NaCl salt-matrix indicates a loose structure. On the contrary, a good spherical shape was observed for the spherical $\text{Fe}_{50}\text{Ni}_{50}$ powders, as shown in Figure 2c,d. The maximum and minimum of size distribution for the spherical alloy powders were about $40\ \mu\text{m}$ and less than $10\ \mu\text{m}$, respectively. The result confirmed that liquid $\text{Fe}_{50}\text{Ni}_{50}$ alloy de-wets from the metalloidal ultrafine alumina powder surface had not merged together, suggesting that this strategy had feasibility using alumina as solid dispersant to segregate the raw material particles. Many previous researchers have reported that alumina particles were used to separate molten metal droplets and prevent their adjoining [16]. Considering the chemical stability at high temperatures, low density, easy separation from the metal powder, and low cost, ultrafine alumina powder was chosen as the solid powder material. In fact, the de-wetting of the liquid metal on a solid medium surface played an important role. The de-wetting, partial wetting and spreading of liquid metal droplets on a solid surface has been reported by many previous works. The high liquid metal surface energy draws into itself on contact with the smaller surface energy for alumina to decrease the system's free energy. The surface energy is generally lower for alumina than the pure Fe surface tension of $1850\ \text{mJ}/\text{m}^2$ and pure Ni surface tension of $1760\ \text{mJ}/\text{m}^2$. Furthermore, the contact angle of liquid Iron and Nickel on Al_2O_3 was 121 and 128 degree, respectively [17]. As in Young's theory, a contact angle above 90° generally indicates that the alloy droplet de-wets from the solid surface. However, it depends on many factors like the metal-metalloid interaction strength, surface energy, mixing energy and mixing entropy [18–20].

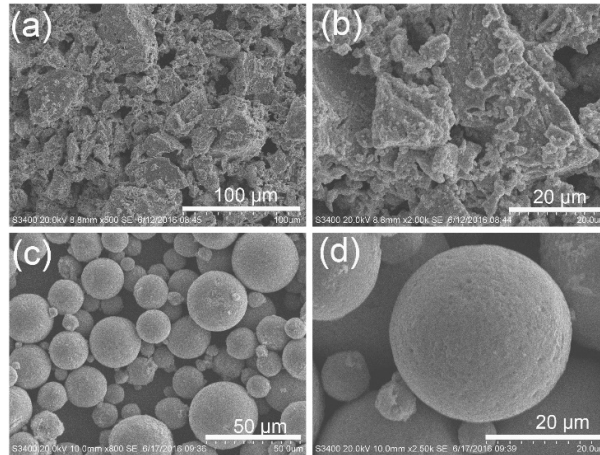


Figure 2. SEM micrographics of (a),(b) prealloy powders reduced at 973 K and (c),(d) spherical $\text{Fe}_{50}\text{Ni}_{50}$ alloy powders fabricated at 1823 K.

The composition analysis of spherical $\text{Fe}_{50}\text{Ni}_{50}$ powders was described by the EDS spectrum of the surface and the cross-sectional image, as shown in Figure 3. Comparing the EDS result of the surface with the inside of the spherical particle, it was confirmed that the impurity alumina phase enriched the spherical particle surface with Al elements detected in the surface and not in the inside shown in Table 1. In addition, the cross-sectional SEM images show that there are no pores and bulk inclusions in the internal region of the spherical particles, as shown in Figure 4c. Furthermore, the element mapping in Figure 3e,f reveals an even distribution of Fe and Ni. The result suggested that the inclusions had not deposited into the inside of liquid alloy droplet, due to de-wetting of the interface between metal droplets and metalloid alumina powders. Some previous research reports the fabrication of Fe-Ni/ Al_2O_3 metal-ceramic materials via the heterogeneous precipitation–thermal reduction process showed different results [21,22]. The key difference is that the annealed temperature of Fe-Ni powders was 973 K but annealed at 1823 K in our experiment, which led the molten Fe-Ni alloy droplet to phase separation from alumina powders. Previous researchers show that liquid alloy with high surface energy draws into itself when contacted with the smaller surface energy (e.g., graphite, SiO_2 and glass) for decreasing the free energy of the system in a nonreactive system, such as liquid metal and metalloid [13,23,24]. But if there exists some reactant in the interface, the spheroidality of the droplet will become more difficult, resulting in the spreading of the wetting line on solid surface for decreasing the system's free energy. The spherical $\text{Fe}_{50}\text{Ni}_{50}$ alloy powders in our work were successfully synthesized using the de-wetting of liquid-solid interface ($\text{Fe}_{50}\text{Ni}_{50}$ /alumina).

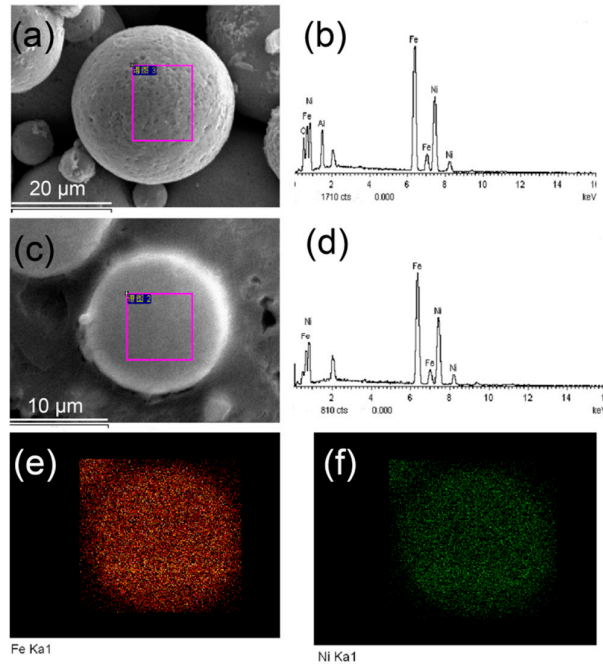


Figure 3. SEM morphology and energy dispersive spectrometer (EDS) of the spherical alloy particle for (a),(b) surface (c),(d) cross-section (e),(f) elemental mapping of cross-section.

Table 1. Composition ratios of Fe and Ni in the spherical alloy sample.

Element	Surface of Particle		Cross-Section of Particle	
	at. %	wt. %	at. %	wt. %
Fe	34.78	43.06	50.56	49.31
Ni	32.96	42.90	49.44	50.69
O	21.59	7.66	-	-
Al	10.67	6.39	-	-

Figure 4 shows XRD patterns and particle size distribution of the $\text{Fe}_{50}\text{Ni}_{50}$ alloy powders. The amorphous nickel hydroxide and iron hydroxide precursors were obtained by using the heterogeneous precipitation, confirmed by the XRD patterns in Figure 4a. From the XRD patterns of the pre-alloy $\text{Fe}_{50}\text{Ni}_{50}$ powder in Figure 4b, only three diffraction peaks are observed in the range of $15\text{--}85^\circ$, which can be assigned to the (111), (200) and (220) phases of FCC (Fe, Ni) alloy (JCPDS No.03-1209). XRD patterns have no peaks of NaCl, indicating that the NaCl salt has been removed. This result is basically consistent with previous reports about $\text{Fe}_{50}\text{Ni}_{50}$ alloy fabricated via salt-matrix utilization [10]. However, a trace amount of the impurity alumina phase was found in the main phase of spherical $\text{Fe}_{50}\text{Ni}_{50}$ alloy powders in Figure 4c even though ultrasonic coupled with magnetic separation in aqueous solution was used to collect the spherical powders. These results show that the spherical Fe-Ni powders are composite powders with alumina insulation coatings. It is in accord with the observation of surface EDS analysis and cross-sectional micrographics that the impurity alumina mainly enriched on the surface of spherical $\text{Fe}_{50}\text{Ni}_{50}$ alloy particles, not on the inside.

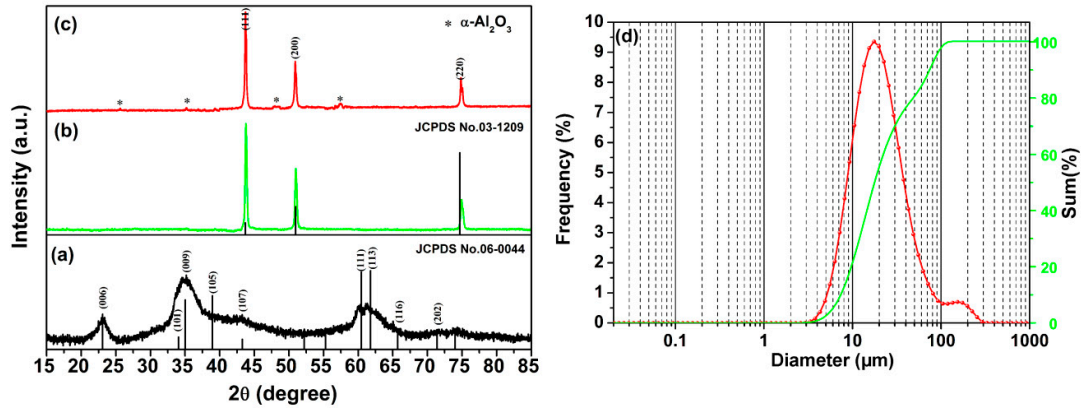


Figure 4. XRD patterns: (a) Mixture metal oxides, (b) prealloy powder reduced at 973K and (c) spherical alloy powder fabricated at 1823 K, (d) particle size distribution of spherical $\text{Fe}_{50}\text{Ni}_{50}$ alloy powder.

Figure 4d shows the size-distribution of particle for spherical $\text{Fe}_{50}\text{Ni}_{50}$ alloy powders annealing at 1823 K. The size distribution at 10%, 50% and 90% of the particles were represented using the volumetric diameters d_{10} , d_{50} and d_{90} , respectively. The d_{10} , d_{50} and d_{90} were smaller than the stated diameter. The size of d_{50} was 20 μm for the as-fabricated spherical alloy powder, which agreed well with the SEM images. Similar to the conventional “solution solvent”, alumina powder presented a new “solid solvent” to some extent.

Figure 5 shows the room temperature magnetic hysteresis loop of the pre-alloy and spherical $\text{Fe}_{50}\text{Ni}_{50}$ alloy powders. The magnetic parameter can be obtained from the curves in Table 2. The saturation magnetizations of pre-alloy and spherical $\text{Fe}_{50}\text{Ni}_{50}$ alloy powders were 131.6 emu/g and 119.4 emu/g, and the corresponding coercivity values were 4.83 Oe and 3.86 Oe, respectively. It was seen that the saturation magnetization of spherical alloy powder was lower than the pre-alloy powder directly reduced from oxides. However, the spherical $\text{Fe}_{50}\text{Ni}_{50}$ powders exhibited an improvement soft magnetic property. The slight decrease of saturation magnetization of spherical $\text{Fe}_{50}\text{Ni}_{50}$ alloy powders can be attributed to the phase composition and microstructure. The non-magnetic oxides on the surface of the spherical alloy powder were easy to decrease magnetic phase.

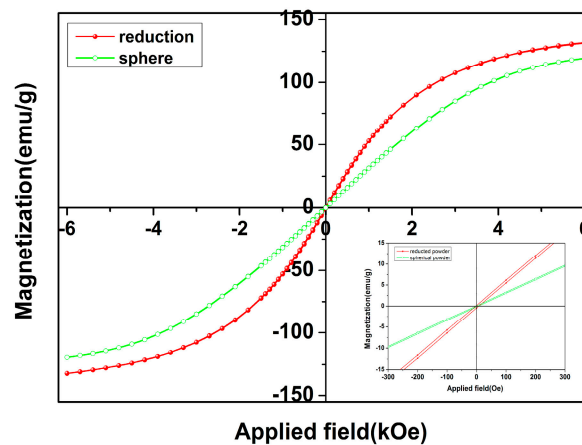


Figure 5. M-H hysteresis loop curve of pre-alloy and spherical $\text{Fe}_{50}\text{Ni}_{50}$ alloy powder. Inset: Enlarged view of coordinates.

Table 2. The magnetic parameter of the reduced pre-alloy powders and the spherical alloy powders for comparison.

Sample	Reduced with Salt Matrix at 973 K	Spheroidizing with Alumina at 1823 K
Ms(emu/g)	131.6	119.4
Mr(emu/g)	0.14	0.05
Hc(Oe)	4.83	3.86

4. Conclusions

Spherical Fe₅₀Ni₅₀ alloy powders were successfully obtained by the reduction of mixture oxides coupled with the in-situ interface de-wetting between liquid Fe₅₀Ni₅₀ alloy and alumina. After hydrogen reduction and heat treatment, the SEM images of alloy powders exhibited a spherical shape, confirming that liquid alloy de-wets from the alumina surface. There were no pores or bulk inclusions in the internal region of the spherical particles, confirming by the cross-sectional SEM images. Furthermore, the element mapping shows that Fe and Ni are evenly distributed. Furthermore, the surface alumina powders can play as the electrical insulation coatings. Magnetic characteristics of alloy powders showed a slight decrease of saturation magnetization of spherical powders than that of pre-alloy powders due to the alumina coating. Our strategies can provide a novel route for fabricating high-quality spherical Fe₅₀Ni₅₀ alloy powders to serve the functional application in soft magnetic cores.

Author Contributions: X.S. conceived the project and synthesized the material; X.S. and C.L. performed the electrochemistry experiments; X.S. and C.L. performed the microscopic study; X.S. and C.L. organized the data and wrote the main manuscript text; C.L. and W.Z. modified the manuscript. All authors have given approval to the final version of the manuscript.

Funding: This research was funded by the National Natural Science Foundation, grant number 51801097, and the Industrial Innovation of Applied Fundamental Research, grant number JC2018022 and the Fundamental Research Funds for the Central Universities.

Conflicts of Interest: The authors declare no conflict of interest.

References

- Meng, X.; Shen, X. Preparation of FeCo-, FeNi- and NiCo-alloy coated cenosphere composites by heterogeneous precipitation. *Particuology* **2012**, *10*, 334–338.
- Godec, M.; Mandrino, D.; Sustarsic, B.; Jenko, M. Surface and electrical studies of Fe-Si-B powders for soft magnetic applications. *Surf. Interface Anal.* **2002**, *34*, 346–351.
- Feng, Y.; Qiu, T. Preparation, characterization and microwave absorbing properties of FeNi alloy prepared by gas atomization method. *J. Alloy. Compd.* **2012**, *513*, 455–459.
- Xu, Z.; Jin, C.; Xia, A.; Zhang, J.; Zhu, G. Structural and magnetic properties of nanocrystalline nickel-rich Fe–Ni alloy powders prepared via hydrazine reduction. *J. Magn. Magn. Mater.* **2013**, *336*, 14–19.
- Dong, S.; Song, B.; Zhang, X.; Deng, C.; Fenineche, N.; Hansz, B.; Liao, H.; Coddet, C. Fabrication of FeSiB magnetic coatings with improved saturation magnetization by plasma spray and dry-ice blasting. *J. Alloy. Compd.* **2014**, *584*, 254–260.
- Fan, X.A.; Wang, J.; Wu, Z.; Li, G. Core-shell structured FeSiAl/SiO₂ particles and Fe₃Si/Al₂O₃ soft magnetic composite cores with tunable insulating layer thicknesses. *Mater. Sci. Eng. B* **2015**, *201*, 79–86.
- Azizi, A.; Sadrnezhaad, S.K. Synthesis of Fe–Ni nano-particles by low-temperature hydrogen reduction of mechanically alloyed Ni-ferrite. *J. Alloy. Compd.* **2009**, *485*, 484–487.
- Shen, X.Q.; Jing, M.X.; Li, W.X.; Li, D.H. Fabrication of Fe-, Ni- and FeNi-coated Al₂O₃ core-shell microspheres by heterogeneous precipitation. *Powder Technol.* **2005**, *160*, 229–233.
- Mirhoseini, F.; Bateni, A.; Firoozi, S. Gas phase synthesis of Ni₃Fe nanoparticles by magnesium reduction of metal chlorides. *Powder Technol.* **2012**, *228*, 158–162.
- Azizi, A. Worthwhile effects of salt-matrix reduction on shape, morphology and magnetic properties of FeNi nanoparticles. *Mater. Sci. Eng. B* **2011**, *176*, 1517–1520.
- Lei, C.; Huang, H.; Huang, Y.; Cheng, Z.; Tang, S.; Du, Y. In-situ de-wetting assisted fabrication of spherical Cu-Sn alloy powder via the reduction of mixture metallic oxides. *Powder Technol.* **2016**, *301*, 356–359.

12. Feng, Y.; Qiu, T. Enhancement of electromagnetic and microwave absorbing properties of gas atomized Fe-50wt%Ni alloy by shape modification. *J. Magn. Magn. Mater.* **2012**, *324*, 2528–2533.
13. Berkowitz, A.E.; Harper, H.; Smith, D.J.; Hu, H.; Jiang, Q.; Solomon, V.C.; Radousky, H.B. Hollow metallic microspheres produced by spark erosion. *Appl. Phys. Lett.* **2004**, *85*, 940.
14. Habenicht, A.; Olapinski, M.; Burmeister, F.; Leiderer, P.; Boneberg, J. Jumping nanodroplets. *Science* **2005**, *309*, 2043–2045.
15. Giermann, A.L.; Thompson, C.V. Solid-state dewetting for ordered arrays of crystallographically oriented metal particles. *Appl. Phys. Lett.* **2005**, *86*, 121903.
16. Pournaderi, S.; Mahdavi, S.; Akhlaghi, F. Fabrication of Al/Al₂O₃ composites by in-situ powder metallurgy (IPM). *Powder Technol.* **2012**, *229*, 276–284.
17. Humenik, M., Jr.; Kingery, W.D. Metal-ceramic interactions: III, surface tension and wettability of metal-ceramic systems. *J. Am. Ceram. Soc.-Humenik Kingery* **1954**, *37*, 18–23.
18. Batyrev, I.G.; Kleinman, L. In-plane relaxation of Cu(111) and Al(111)/ α -Al₂O₃(0001) interfaces. *Phys. Rev. B* **2001**, *64*, doi:10.1103/PhysRevB.64.033410.
19. Zhou, X.B.; de Hosson, J.T.M. Reactive wetting of liquid metals on ceramic substrates. *Acta Mater.* **1996**, *44*, 421–426.
20. Oshanin, G.; de Coninck, J.; Cazabat, A.M.; Moreau, M. Dewetting, partial wetting, and spreading of a two-dimensional monolayer on solid surface. *Phys. Rev. E* **1998**, *58*, R20.
21. Silva, H.; Nielsen, M.G.; Fiordaliso, E.M.; Damsgaard, C.D.; Gundlach, C.; Kasama, T.; Chorkendorff, I.B.; Chakraborty, D. Synthesis and characterization of Fe–Ni/ γ -Al₂O₃ egg-shell catalyst for H₂ generation by ammonia decomposition. *Appl. Catal. A Gen.* **2015**, *505*, 548–556.
22. Chen, M.; Gao, M.; Dang, F.; Wang, N.; Zhang, B.; Pan, S. Tunable negative permittivity and permeability in FeNiMo/Al₂O₃ composites prepared by hot-pressing sintering. *Ceram. Int.* **2016**, *42*, 6444–6449.
23. Passerone, A.; Muolo, M.L.; Passerone, D. Wetting of group IV diborides by liquid metals. *J. Mater. Sci.* **2006**, *41*, 5088–5098.
24. Yasinskaya, G. The wetting of refractory carbides, borides, and nitrides by molten metals. *Sov. Powder Metall. Metal Ceram.* **1966**, *5*, 557–559.



© 2019 by the authors. Licensee MDPI, Basel, Switzerland. This article is an open access article distributed under the terms and conditions of the Creative Commons Attribution (CC BY) license (<http://creativecommons.org/licenses/by/4.0/>).